Desalination and Water Treatment
www.deswater.com

doi: 10.5004/dwt.2021.27557

234 (2021) 22–30
September

Brine outfall modeling of the proposed desalination plant of Fortaleza, Brazil

Silvano Porto Pereira*, Paulo Cesar Colonna Rosman, José Luis Sánchez-Lizaso, Iran Eduardo Lima Neto, Rodrigo Amado Garcia Silva, Melissa Rodrigues

Companhia de Água e Esgoto do Ceará (CAGECE), Lauro Vieira Chaves Street, 1030, 60.422-901, Fortaleza, Brazil, Tel. +55 85 3101-1895; emails: silvanopereira@terra.com.br (S.P. Pereira), pccrosman@gmail.com (P.C.C. Rosman), jl.sanchez@ua.es (J.L. Sánchez-Lizaso), iran@deha.ufc.br (I.E. Lima Neto), rodrigoamado@oceanica.ufrj.br (R.A. Garcia Silva), melissa.rodrigues_@oceanica.ufrj.br (M. Rodrigues)

Received 25 January 2021; Accepted 28 June 2021

ABSTRACT

Seawater desalination has been considered an important solution for the water scarcity in coastal areas. Brazil has an 8,000 km long coastline where population and tourism have grown tremendously in the last years. Fortaleza is the fifth-largest city in Brazil with nearly 2.6 million inhabitants, representing an important economic, recreational and touristic area in the Northeast. In addition, it is the city with the greatest gross domestic product (GDP) in the region, and ninth in the country. In the past 7 y, the dams that supply water to the Metropolitan Region of Fortaleza have undergone droughts. This led the government to start a large-scale seawater desalination project that shall produce desalinated water at about 1.0 m^3/s, for which plant location, water intake and brine disposal studies were performed. The most common environmental impact associated with desalination plants is the high concentration brine discharge. Aiming to evaluate the possible impact of such discharges, environmental modeling has become an important tool for projects, environmental management and studies, due to the complexity of these environments. With this tool, it is possible to integrate a large number of variables and processes to obtain a dynamic vision of those systems and evaluate present and future conditions. This work presents outcomes from brine discharge modeling in the water quality of the coast of Fortaleza, in particular, increased salinity, using Visual Plumes to evaluate near-field dilution and SisBaHiA (Environmental Hydrodynamic Base System) software to generate a hydrodynamic model and evaluate far-field dilution. Hydrodynamic models, forced by wind and tide, were coupled with a wave propagation model and then used in a Lagrangian transport model, which was fed by the outcomes of the near-field model. From the results generated, it was identified that the installation of the proposed desalination plant in Fortaleza does not compromise water quality and is consistent with the results reported in the literature, regarding the reduced impact caused by the disposal of this type of concentrate.

Keywords: Desalination discharge; Brine dilution; Plume dispersion

1. Introduction

In the last decades, water availability for human consumption has been drastically reduced in many regions of the planet. The State of Ceará, in the Northeastern region of Brazil, is characterized by long cyclical periods of rainfall shortage, being the subject of numerous studies that seek a greater understanding of its variability and associated natural mechanisms, but its behavior is not yet fully understood.

In order to guarantee the necessary water security considering climatic uncertainties, water supply alternatives

* Corresponding author.

have been sought to strengthen the State's water matrix, especially that of the Metropolitan Region of Fortaleza, as it is responsible for the greater human consumption water demand and is heavily dependent on water transfer from distant watersheds. Seawater desalination has been mentioned for a long time as a possible source to diversify the State's water matrix, and it is currently in the process of contracting the first large seawater desalination plant in Brazil with a production capacity of about 1.0 m^3/s to meet part of the water demand in Fortaleza, which currently has a population of over 2.6 million inhabitants. It is expected to start construction in 2022 and its completion in 2024.

During the desalinated water production process, regardless of the technology adopted, there is always a salt concentrate stream that needs to be given an appropriate destination. Although there are different disposal options for this concentrate, such as discharge into the sea, deep well injection, evaporation ponds, dilution with domestic sewage or production of salts and other minerals, the seawater discharge option is one of the most adopted for economic reasons [1], being the selected method for the specific case of the aforementioned plant.

As a reference for international criteria and standards on saline concentrate disposal from desalination plants, in 2012 the California Water Resources Control Board [2] presented a technical review for this type of discharge, including recommendations and disposal criteria, which are presented in Table 1. Although there is considerable variation in the specificities of each regulation, most share two key elements: a salinity limit and a compliance distance. The limit salinity is usually adopted as an increase not exceeding the range between 1 and 4 ppt in relation to the environmental salinity; however, in some cases, absolute values or a minimum acceptable dilution are adopted. The compliance limit, on the other hand, is adopted as the limit of the mixing zone, which is usually specified in terms of a fixed distance from the discharge point that varies between 50 and 300 m.

The mixing process of effluents discharged from a marine outfall consists of near-field and far-field mixing processes, which occur at different spatial and time scales [13]. The first basically depends on environmental conditions (water turbulence, current speed and thermal and hyaline stratification) and characteristics of the diffusers and effluents discharged. In this area, the initial stream characteristics, determined by outlet geometry, discharge conditions and the environment (in particular the density differences), have a direct influence on the jet trajectory and the dilution process. As the stream moves away from the discharge point, the diffusers' geometric characteristics begin to have less influence over the dilution process, starting a second phase in the area called the far-field, where the plume becomes a density current that moves across the seabed at a small dilution rate (Fig. 4), unlike the near-field region. Logically, the more diluted the stream is in the near-field region complemented by a correct discharge configuration, the more diluted it will be in far-field region, thus reducing the affected area [14].

Aiming to predict the behavior of the saline concentrate released to the sea, computational models can be applied as an essential tool for the environmental assessment of desalination projects, considering different concentrate properties, diffuser configurations and marine conditions.

In most models used for this purpose, three different approaches are normally considered [15]: (I) dimensional analysis of the main processes, which can be tested experimentally; (II) the integration of ordinary differential equations (integral models); and (III) the numerical solution of partial differential equations with less simplifications (computational fluid dynamics – CFD).

Table 1
Guidelines and salinity standards for the disposal of saline concentrate from desalination plants through marine outfalls

Region/Authority	Salinity limit	Compliance point[a]	Source
Carlsbad, CA	≤40 ppt	305 m	WateReuse association [3]
Huntington Beach, CA	≤40 ppt (as a dilution of 7.5:1)	305 m	
Spain	<38.5 ppt	Seagrass limit	Sanchez-Lizaso et al. [4]
US EPA	Increase ≤4 ppt		US EPA [5]
Western Australia Guidelines	Increase <5%		Bleninger et al. [6]
Abu Dhabi	Increase ≤5%	Mixing zone boundary	
Oman	Increase ≤2 ppt	300 m	Sultanate of Oman [7]
Gold Coast, Australia	Increase ≤2 ppt	120 m	GCD Alliance [8]
California Environmental Protection Agency	Increase ≤2 ppt	100 m	SWRCB [9]
Perth, Australia/Western	Increase ≤1.2 ppt	50 m	WEC [10]
Australia EPA	Increase ≤0.8 ppt	1,000 m	
Sydney, Australia	Increase ≤1 ppt	50–75 m	ANZECC [11]
Okinawa, Japan	Increase ≤1 ppt	Mixing zone boundary	Okinawa Bureau for Enterprises [12]

[a]relative to the discharge;
Modified from [2].

Software such as CORMIX [16], Visual Plumes [17] and VISJET [18], which are widely used in simulations of positive buoyancy jets, can also be used in the case of negative buoyancy to predict concentrate behavior in the near field area [15]. Since these models do not have their own hydrodynamic modeling tools, they require data from marine currents operating in the area as main input parameters, whether obtained through measurements or produced externally by other models.

This article performs simulations of the effluent discharge from the proposed desalination plant of Fortaleza, Brazil, integrating its near and far-fields. The Visual Plumes model system was used to assess the near field and the SisBaHiA (Environmental Hydrodynamic Base System) software [19] for the definition of local hydrodynamic, forced by winds, tides and waves. Subsequently, a SisBaHiA Lagrangian transport model, coupled to the hydrodynamic model and fed by near-field results from the Visual Plumes model, was used to reproduce far-field salt plume behavior.

2. Material and methods

2.1. Location and description of the Fortaleza Desalination Plant and its brine discharge

The desalination plant will be located at Praia do Futuro, in Fortaleza, State of Ceará, Brazil and shall dispose of 1.23 m^3/s of brine by a submarine outfall. The pipeline shall have a diameter of 1,200 mm, be located at 1,200 m from the shoreline and have 8 diffusers in its final 25 m, each with 280 mm in diameter, located at a depth of 12 m. The diffusers shall be a single port type, 45° vertical angle, 270° horizontal angle (parallel to the shoreline) and one meter high. The diffuser location is presented in Fig. 1 (UTM coordinates zone 24S; 561,527m E and 9,587,828m N), where the plant and pipeline locations can be observed.

2.2. Computing tools

The Visual Plumes software UM3 model [8] was used to evaluate the initial dilution values and near-field extensions, considering, at 1-h intervals, the intensities and directions of the marine currents exhibited at the location foreseen for outfall implementation, in two different scenarios described below. The demonstrated currents were generated by the hydrodynamic model implemented in the SisBaHiA software, forced by winds and tides while coupled to a wave propagation model. The concentrations obtained in the near-field were then used to feed the Lagrangian transport model, also implemented in SisBaHiA, with the latter coupled to the previously used hydrodynamic model.

SisBaHiA software is a process-based modeling system enhanced and supported by the Federal University of Rio de Janeiro, developed for application in studies regarding free surface water bodies (e.g., Pereira et al., [20]; Feitosa et al. [21]; Sawakuchi et al. [22]; Peixoto et al. [23]; Barros and Rosman [24]; Silva et al. [25]; IAEA [26]; Horita and Rosman [27]). Three modules of SisBaHiA have been applied in this research: a hydrodynamic model, a wave propagation model and a Lagrangian transport model. For the purpose of this research, one adopted the option of a hydrodynamic model that solves the 2DH shallow water momentum conservation Eqs. (1) and (2), and the mass conservation Eq. (3), for incompressible flow with homogeneous density in a finite element discretization scheme:

Fig. 1. Map showing the desalination plant, its outfall position (orange line) and water intake (blue).

$$\frac{\partial u}{\partial t}+u\frac{\partial u}{\partial x}+v\frac{\partial u}{\partial y}=-g\frac{\partial \zeta}{\partial x}+\frac{1}{\rho_0(\zeta+h)}\left(\frac{\partial\left[(\zeta+h)\hat{\tau}_{xx}\right]}{\partial x}+\frac{\partial\left[(\zeta+h)\hat{\tau}_{xy}\right]}{\partial y}\right)+\frac{1}{\rho_0(\zeta+h)}\left(\tau_x^s-\tau_x^B\right)-\frac{1}{\rho_0(\zeta+h)}\left(\frac{\partial S_{xx}}{\partial x}+\frac{\partial S_{xy}}{\partial y}\right) \quad (1)$$

$$\frac{\partial v}{\partial t}+u\frac{\partial v}{\partial x}+v\frac{\partial v}{\partial y}=-g\frac{\partial \zeta}{\partial y}+\frac{1}{\rho_0(\zeta+h)}\left(\frac{\partial\left[(\zeta+h)\hat{\tau}_{xy}\right]}{\partial x}+\frac{\partial\left[(\zeta+h)\hat{\tau}_{yy}\right]}{\partial y}\right)+\frac{1}{\rho_0(\zeta+h)}\left(\tau_y^s-\tau_y^B\right)-\frac{1}{\rho_0(\zeta+h)}\left(\frac{\partial S_{yx}}{\partial x}+\frac{\partial S_{yy}}{\partial y}\right) \quad (2)$$

$$\frac{\partial(\zeta+h)}{\partial t}+\frac{\partial u(\zeta+h)}{\partial x}+\frac{\partial v(\zeta+h)}{\partial y}=0 \quad (3)$$

In Eqs. (1)–(3) $u(x, y, t)$ and $v(x, y, t)$ are the 2DH velocity components in x and y, respectively; g is the gravity acceleration; $z = \zeta(x, y, t)$ and h are the free surfaces and the bathymetry, respectively, referred to the mean low water spring; ρ_0 is the reference water density; $\hat{\tau}_{xx}$, $\hat{\tau}_{xy}$, $\hat{\tau}_{yx}$ and $\hat{\tau}_{yy}$ are the turbulent shear stresses; τ^S and τ^B are the shears stresses on the free surface and on the bottom, respectively; and S_{xx}, S_{xy}, S_{yx} and S_{yy} are the wave radiation stresses calculated by the wave model. Note that the wave model of SisBaHiA is based on REF/DIF 1 version 3.0 [28].

In turn, the Lagrangian model of SisBaHiA considers three stages for the transport process, involving advection and dispersion of the particles and, additionally, the diffusion in relation to the center of mass of each respective particle. The mass transport of the saline concentrate is simulated by the movement of a given number of particles randomly released within a source region, which are transported by the currents generated by the hydrodynamic model, disregarding the kinetic effects for this specific case. Details regarding the SisBaHiA Lagrangian model can be found in Horita and Rosman [27].

2.3. Study area

Fig. 2 shows the bathymetry and grid domain of the area covered by the hydrodynamic and transport models. The grid has an area of 285 km^2, containing 1,980 quadratic elements and 8,454 nodes.

Bathymetric and surface roughness data were retrieved from charts DHN #701 (1:130,000) and DHN #710 (1:50,000) produced and updated in 2011 by the Brazilian Navy's hydrography and navigation department. The bathymetric map in Fig. 1 was based on 2,395 depth points of the nautical charts, producing a 30 × 30 m grid for interpolation. The depth from each node was subsequently entered into the SisBaHiA database. The roughness data was based on 143 points comprising different soil types converted into rugosity.

2.4. Tides and winds

The model was forced with the local tides along the open boundary and wind stress over the domain. Fifty tidal harmonic constituents were calculated by a tide gauge installed in the Fortaleza harbor, with a basis on 6-month water level records (from the 1st of June to the 30th of November of 2008). Local tides are fully semidiurnal (tidal form number: 0.2). The mean spring and neap tides in the area are 1 and 3 m high, respectively.

Wind data were recorded every 10 min by a 15 m high weather station close to the beach (–3.718° and –38.536°). According to Pereira [29], the most frequent winds in the area are easterly directed, ranging from 5 to 8 m/s in the case of moderate winds, 8 to 10 m/s in the case of strong winds and higher than 10 m/s in the case of gusty winds. To represent the variation of wind conditions in different seasons, the

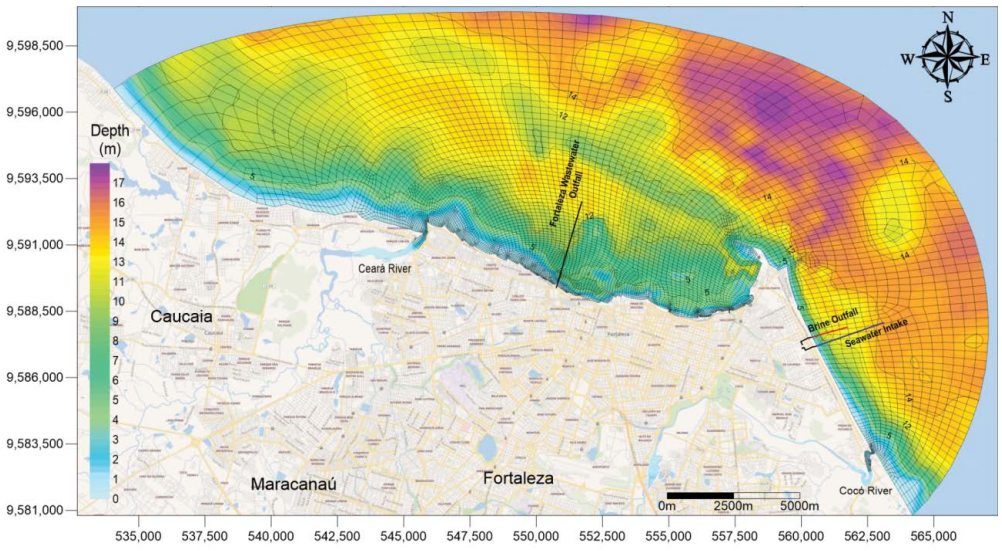

Fig. 2. Study area, showing a grid, depth, the brine outfall on the coast of Fortaleza, Ceará, Brazil.

months of April and November were selected. Fig. 3 shows the wind pattern in the area for the simulated scenarios.

2.5. Currents

Since there are no current measurements done in the target area, wherever the desalination plant's submarine outfall may be installed, measurements already performed in another location by Pereira et al. [20] were used, within the modeling domain selected herein. The purpose was to select the wind characteristics that best display its effects on local currents.

2.6. Waves

Wave propagation methods (WPM) were coupled to the previously calibrated hydrodynamic models. This method considered waves propagated from deep waters to the area of interest. A time series of such deep-water waves was used, characteristic of the months of April and November. The objective of this simulation was to represent general current patterns near the coastline for the random months of April and November under the influence of these waves since coastal current behavior can be quite sensitive to wave incidence.

3. Results and discussion

3.1. Hydrodynamic modeling

As discussed by Pereira et al. [20], the pattern of coastal currents near Fortaleza is primarily determined by winds, with tides playing a minor role. As Fig. 4 shows, coastal currents near Praia do Futuro are always NNW directed. However, the longshore current's direction may change according to wave conditions. Alongshore currents, which are wave-generated currents acting along the wave-breaking zone, are highly dependent on the direction of incident waves.

In the April scenario, the alongshore currents at Praia do Futuro headed SSE most of the time, driven by NNE

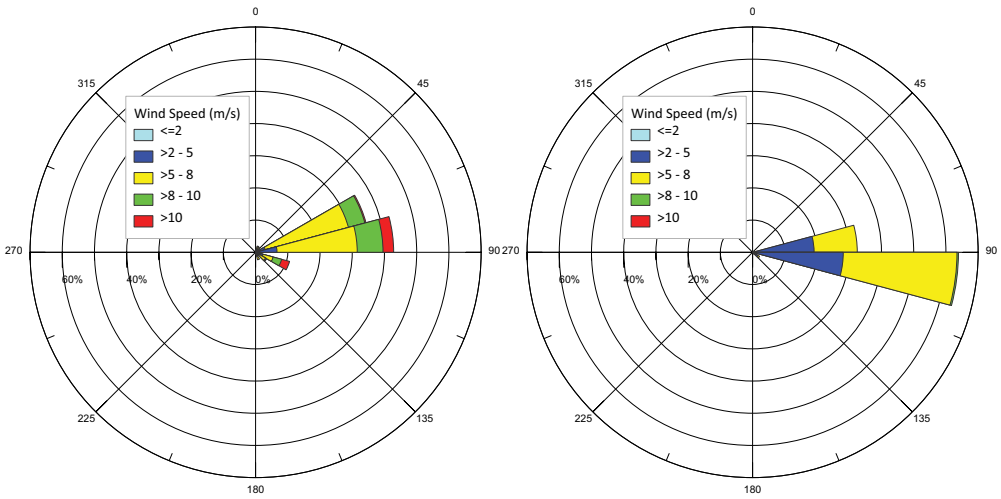

Fig. 3. Wind velocity distribution as a function of wind direction in (A) April 2012 and (B) November 2011.

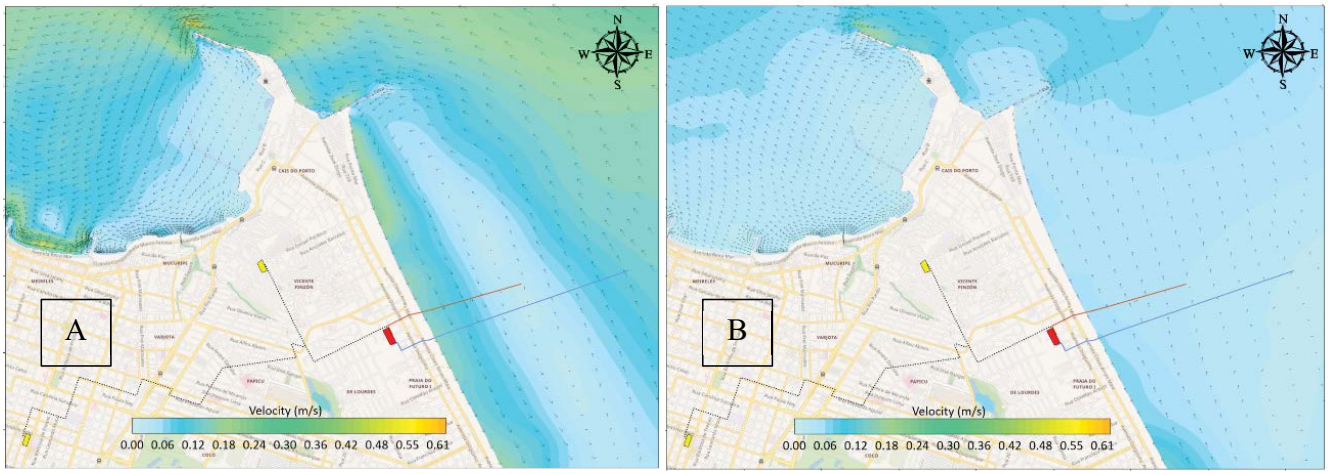

Fig. 4. Coastal currents in April (A), under NNE wave conditions, and in November (B), under E waves conditions. As one may observe, longshore currents are influenced by wave direction, while coastal currents depend only on the winds.

incident waves (Fig. 4A). In the November scenario, the modeled longshore currents were NNW directed all the time.

Fig. 5 depicts the pattern of current magnitude and direction near the water desalination plant outfall for both depicted scenarios. As one may notice, the direction of the currents near the outfall in April may be NNW or SSE, while in November only NNW-directed currents were observed. This behavior reveals that the hydrodynamic circulation near the outfall is not only influenced by wind-driven coastal currents, but also by the action by wave-generated longshore currents. This is consistent with the results of Silva et al. [30] who discuss, in further detail, the April and November hydrodynamic modeling scenario characteristics, as well as the water levels and coastal current calibration processes.

3.2. Near-field modeling

Fig. 6 presents near-field simulations results for April's and November's aforementioned marine conditions. As shown in the figure, the centerline maximum heights reached by the jets emitted by the diffusers, installed at 1 m from the seafloor and at a depth of 12 m, were between 1.7 and 2.1 m away from the discharge point in April and in November. Fig. 6 also shows that the boundaries of the jets display a vertical spread in April greater than that predicted in November, due to the increased variability of current velocities in the former month, as long as the horizontal extents of their centerlines have been more restricted, due to lower current intensities.

According to Palomar et al. [31], the UM3 model is a good alternative to model saline concentrates, although, in stagnant environments, it underestimates jet dimensions. In dynamic environments, however, the authors state that, in accordance with other models and experimental data, the maximum jet heights tend to be shorter as the acting currents are reduced.

When the maximum height is reached, the negatively buoyant jet begins to collapse, continuing the entrainment and dilution processes until it reaches the marine soil, where it spreads horizontally (Fig. 7) as a turbulent density current [32], promoting further dilution while it is advected by the marine currents. Subsequently, the turbulence reduces under the influence of its own density stratification,

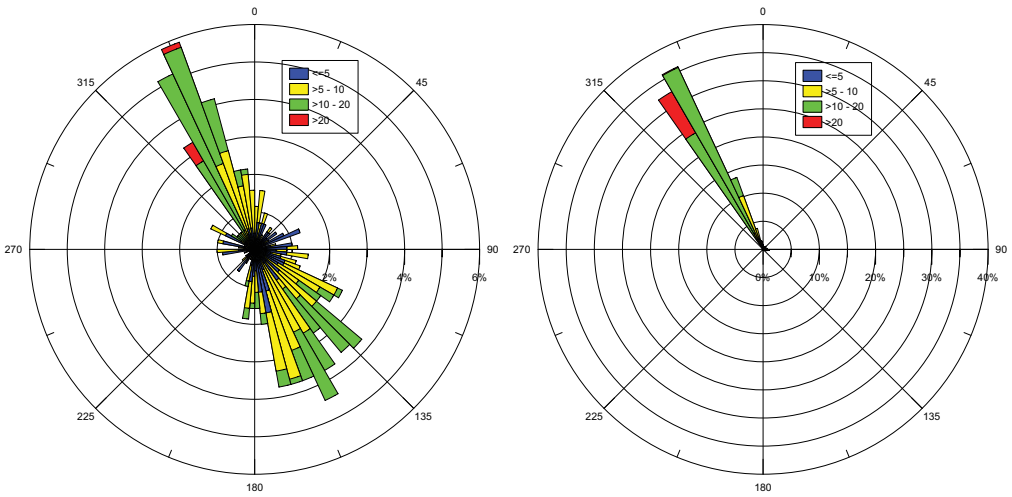

Fig. 5. Coastal currents near the water desalination plant outfall for (A) April-2012 and (B) November-2011.

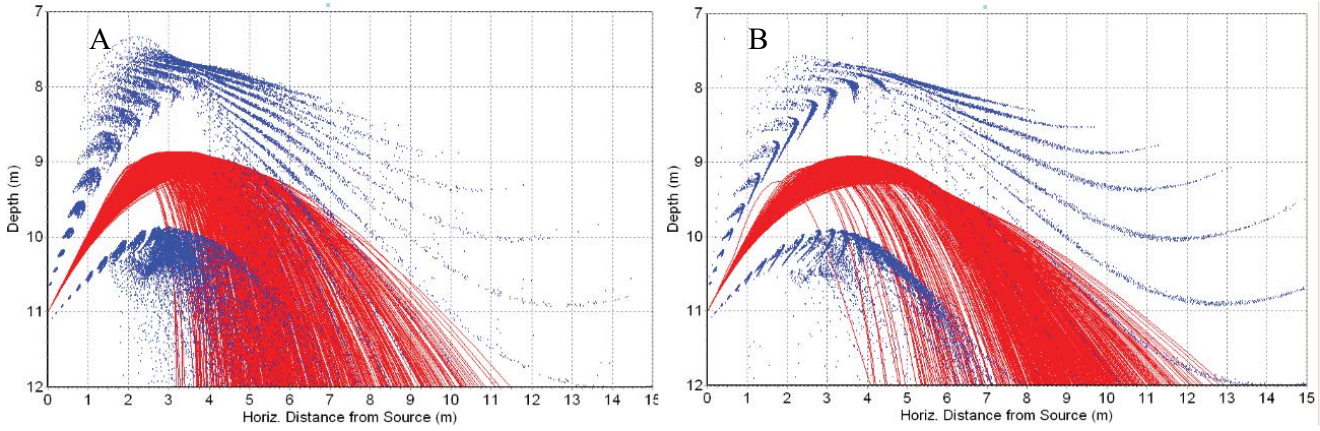

Fig. 6. The behavior of the centerline (lines) and boundaries (dots) of the saline jets in the near field in April (A) and November (B) conditions, with an indication of their vertical and horizontal ranges.

indicating the end of the near field [13], when the formed plume is then passively advected by ambient currents.

The horizontal range, in its turn, was between 3 and 12 m from the original spot in April and between 4 and 13 in November (Figs. 6 and 7), directly proportional to the currents operating on the diffusers. The results also indicated that the exceedance concentration at these points was always less than 3 ppt, already complying with five of the guidelines proposed in Table 1.

Still, regarding the dilution rates found in the near field, Fig. 8 shows the existence of a direct relationship between these and the currents operating on the diffusers. Since marine currents with directions not perpendicular to diffuser positions (Fig. 5) occur in April, even with several directions opposite to their alignment, the effect of the currents is not as accentuated as in November. As a result, the dilution rates observed in April were greater than 10, while in November, they exceeded 15 (Fig. 8).

Considering a 67.27 ppt saline effluent concentration (30.27 above local salinity) in this near-field location, the concentration exceeding the average would be close to only 3 and 2 ppt, respectively to these months, already complying with a good portion of the guidelines presented in Table 1.

The exceeding concentration values achieved in the aforementioned near-field for the months of April and November were then inserted as a source in the SisBaHiA transport model, to assess their distribution around the marine outfall. However, for safety reasons, a very conservative situation was adopted, with the initial dilution established at only 10 times, a value that was surely achieved by

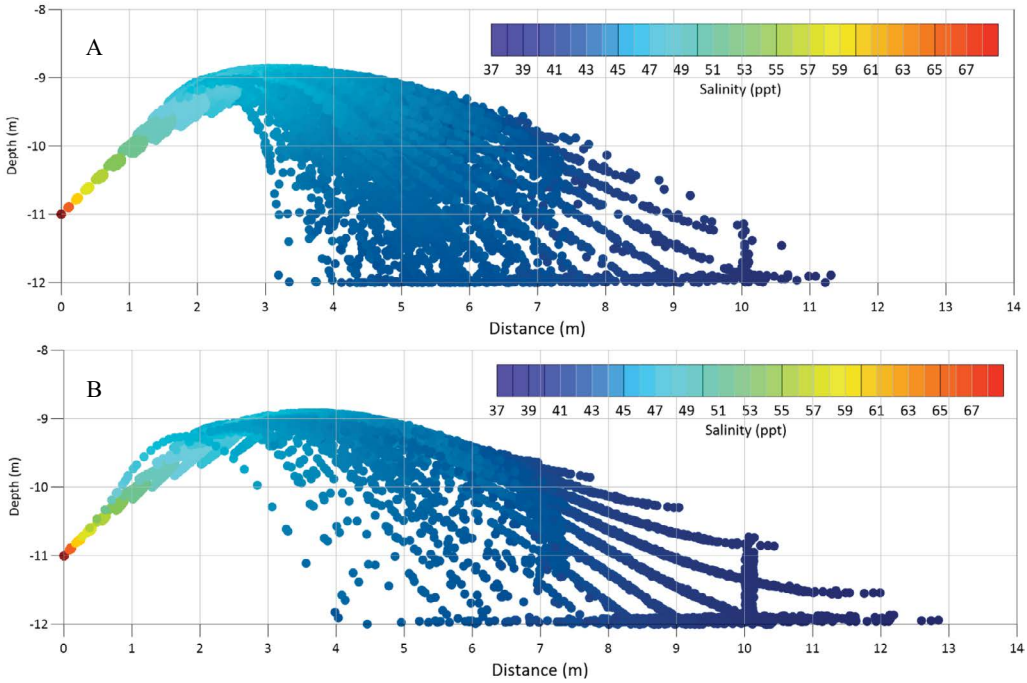

Fig. 7. Estimated salt concentration values along the centerline of effluent jets from the submarine outfall, under the marine conditions of April (A) and November (B).

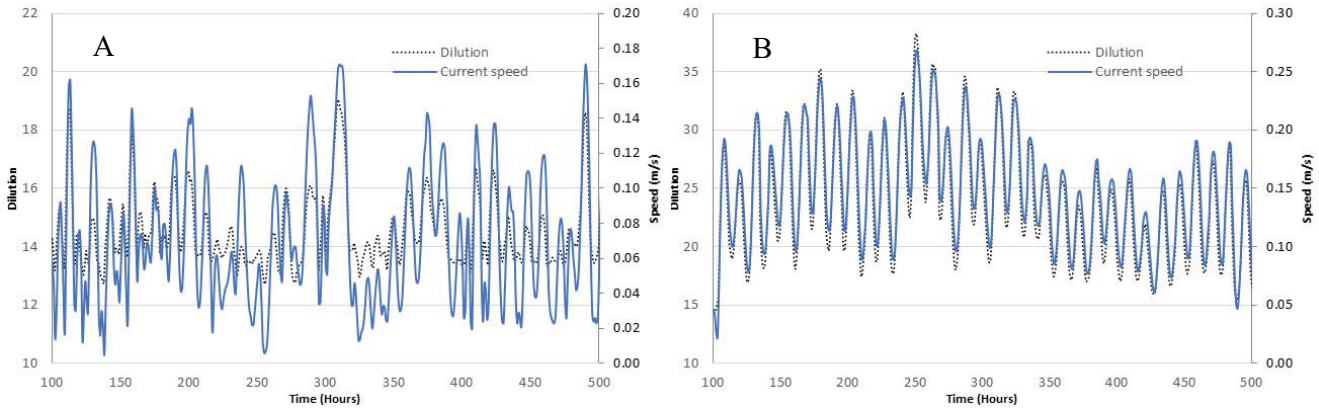

Fig. 8. Expected saline effluent dilution rates when reaching the seabed, under the marine conditions of April (A) and November (B).

the set of diffusers provided. Considering this, the exceeding concentration in the source area was set at 3 ppt in order to feed the SisBaHiA Lagrangian transport model, which is represented in the next topic.

3.3. Far-field modeling

Figs. 9 and 10 present results from simulation periods in November, under the influence of waves from the East, as shown in Fig. 4B, and in April, under the influence of waves from the East-Northeast, as shown in Fig. 4A, causing a concentrate spread according to directions indicated in the map vectors. In these situations, the most restrictive condition displayed in the guidelines presented in Table 1 (0.80 ppt) is reached within an extension of less than 100 m, which is below the compliance distance indicated for this condition (1,000 m).

According to Inan [33], when wind speed decreases, current velocity also decreases, making dilution difficult in the near and far-fields, which is consistent with the results compared here for the months indicated.

When all the hourly results produced for April and November were considered, no surpassing of the less restrictive guideline limits (2 and 4 ppt) was identified. There was also no risk that the saline plume would reach the seawater intake area, which would bring a risk of concentrate recirculation. This result confirms the importance of coupling near and far-field models for such analyses, thus optimizing the design and location.

4. Conclusion

The saline concentrate dispersion model derived from the marine outfall of the proposed desalination plant of Fortaleza, Brazil indicated that the area affected by the saline plume is quite small, increasing local salinity by only 0.8 ppt in an area up to 300 m surrounding the discharge point, meeting the most restrictive international guidelines

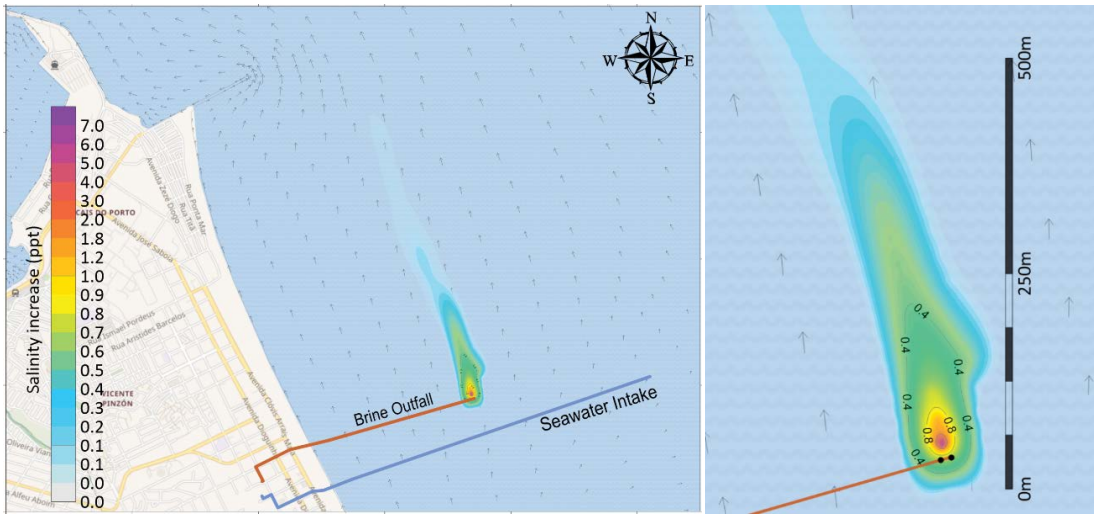

Fig. 9. Increase in salinity (ppt) due to saline concentrate disposal by the outfall, in a given period of November.

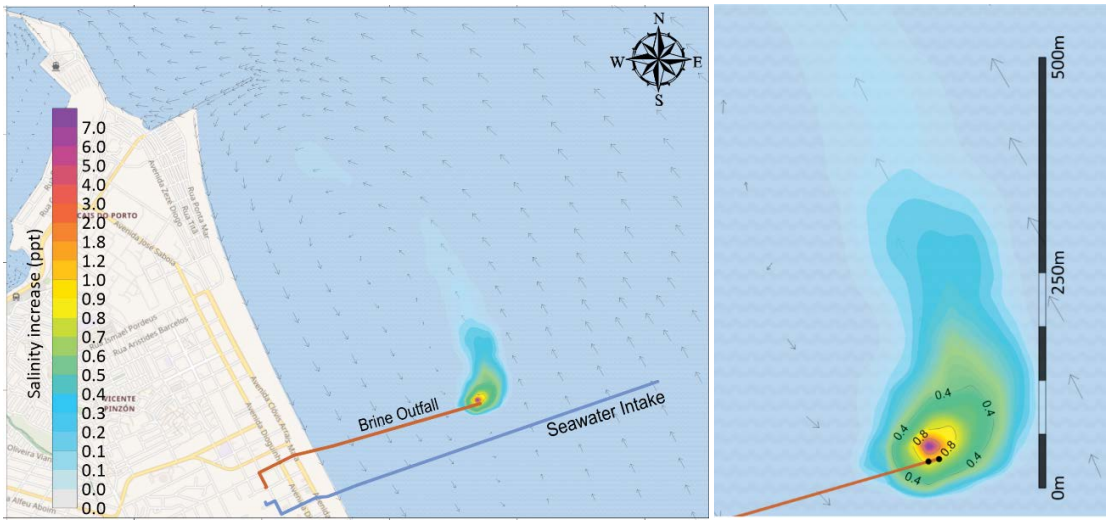

Fig. 10. Increase in salinity (ppt) due to saline concentrate disposal by the outfall, in a given period of April.

reviewed by the California Water Resources Control Board and corresponding to what is practiced by the Western Australian Environmental Protection Authority.

In the case of the less restrictive limits indicated in the above-mentioned guidelines, which are those between 1.85 and 4 ppt, no exceeding risk was identified for April or November, as well as no risk of the plume reaching the seawater intake area.

Despite these results, it is recommended that the model is further calibrated with current measurements performed as close as possible to the disposal site, considering that, due to the absence of measurements in the Praia do Futuro area, the model used herein was previously calibrated with data from currents surrounding the marine outfall of sanitary effluents in Fortaleza.

However, for a preliminary analysis phase, where conservative assumptions were made regarding the underestimation of initial dilutions, the results are consistent with what is reported in the literature regarding the reduced impact caused by the disposal of this type of concentrate.

Overall, this study illustrates the relevance of coupling near and far-field models for optimizing the design and location of marine outfalls.

References

[1] Y. Fernández-Torquemada, A. Carratalá, J.L. Sánchez-Lizaso, Impact of brine on the marine environment and how it can be reduced, Desal. Water Treat., 16 (2019) 27–37.

[2] P. Roberts, S. Jenkins, J. Paduan, D. Schlenk, J. Weis, Management of Brine Discharges to Coastal Waters: Recommendations of a Science Advisory Panel, Environmental Review Panel (ERP), Southern California Coastal Water Research Project (SCCWRP), Technical Report 694, Costa Mesa, CA, 2012.

[3] WateReuse Association, Seawater Concentrate Management, White Paper, 2011.

[4] J.L. Sánchez-Lizaso, J. Romero, J. Ruiz, E. Gacia, J.L. Buceta, O. Invers, Y.F. Torquemada, J. Mas, A. Ruiz-Mateo, M. Manzanera, Salinity tolerance of the Mediterranean seagrass *Posidonia oceanica*: recommendations to minimize the impact of brine discharges from desalination plants, Desalination, 221 (2008) 602–607.

[5] US EPA, Quality Criteria for Water, Gold Book, Office of Water Regulations and Standards, U.S. Environmental Protection Agency, Washington, 1986.

[6] T. Bleninger, G.H. Jirka, S. Lattemann, Environmental Planning, Prediction and Management of Brine Discharges from Desalination Plants, Middle East Desalination Research Center (MEDRC), Muscat, Sultanate of Oman, 2010.

[7] Sultanate of Oman, Ministerial Decision No: 159/2005, Promulgating the Bylaws to Discharge Liquid Waste in the Marine Environment, Ministry of Regional Municipalities, Environment and Water Resources, 2005. Available at: https://omanportal.gov.om/wps/wcm/connect/EN/site/home/gov/gov5/gov53/

[8] GCD Alliance, Material Change of Use Application ERA 16, 19 and 7, Gold Coast Desalination Project, 2006.

[9] SWRCB, California Ocean Plan, 2019.

[10] WEC, Perth Metropolitan Desalination Proposal, Environmental Protection Statement, Prepared by Welker Environmental Consultancy for Water Cooperation, 2002.

[11] ANZECC, Australian and New Zealand Guidelines for Fresh and Marine Water Quality, 2000.

[12] Okinawa Bureau for Enterprises, Environmental Impact Assessment Report for the Seawater Desalination Project in Okinawa, Japan, Executive Summary, 1997.

[13] P.J.W. Roberts, Near Field Flow Dynamics of Concentrate Discharges and Diffuser Design, Environmental Science and Engineering, T.M. Missimer, B. Jones, R.G. Maliva, Eds., Intakes and Outfalls for Seawater Reverse-Osmosis Desalination Facilities, 2015, pp. 369–396.

[14] A. Loya-Fernández, L. Ferrero-Vicente, C. Marco-Méndez, E. Martínez-García, J. Zubcoff, J.L. Sánchez-Lizaso, Comparing four mixing zone models with brine discharge measurements from a reverse osmosis desalination plant in Spain, Desalination, 286 (2012) 217–224.

[15] P. Palomar, J.L. Lara, I.J. Losada, M. Rodrigo, A. Alvárez, Near field brine discharge modelling part 1: analysis of commercial tools, Desalination, 290 (2012) 14–27.

[16] R.L. Doneker, G.H. Jirka, CORMIX-GI systems for mixing zone analysis of brine wastewater disposal, Desalination, 139 (2001) 263–274.

[17] W.E. Frick, Visual Plumes Mixing Zone Modeling Software, Environmental Modelling & Software, v. 19, n. 7–8 (2004) 645–654.

[18] S.K.B. Cheung, D.Y.L. Leung, W. Wang, J.H.W. Lee, V. Cheung, VISJET – A Computer Ocean Outfall Modelling System, Computer Graphics International Proceedings, Geneva, Switzerland, 2000, pp. 75–80

[19] P.C.C. Rosman, Referência Técnica do SisBaHiA, Rio de Janeiro, 2020.

[20] S.P. Pereira, P.C.C. Rosman, C. Alvarez, C.A.F. Schetini, R.O. Souza, R.H.S.F. Vieira, Modeling of coastal water contamination in Fortaleza (Northeast of Brazil), Water Sci. Technol., 72 (2015) 928–936.

[21] R.C. Feitosa, P.C.C. Rosman, T. Bleninger, J.C. Wasserman, Coupling bacterial decay and hydrodynamic models for sewage outfall simulation, J. Appl. Water Eng. Res., 1 (2013) 137–147.

[22] H.O. Sawakuchi, V. Neu, N.D. Ward, M.L.C. Barros, A.M. Valerio, W. Gagne-Maynard, A.C. Cunha, D.F.S. Less, J.E.M. Diniz, D.C. Brito, A.V. Krusche, J.E. Richey, Carbon dioxide emissions along the Lower Amazon River, Front. Mar. Sci., 4 (2017) 76, doi: 10.3389/fmars.2017.00076.

[23] R. dos Santos Peixoto, P.C.C. Rosman, S.B. Vinzon, A morphodynamic model for cohesive sediments transport, Braz. J. Water Res., 22 (2017), doi: 10.1590/2318-0331.0217170066.

[24] M.L.C. Barros, P.C.C. Rosman, A study on fish eggs and larvae drifting in the Jirau reservoir, Brazilian Amazon, J. Braz. Soc. Mech. Sci. Eng., 40 (2018) 62, doi: 10.1007/s40430-017-0951-1.

[25] R.A.G. Silva, M.N. Gallo, P.C.C. Rosman, I.C.M. Nogueira, Tidal inlet short-term morphodynamics analysed trough the tidal prism – longshore sediment transport ratio criterion, Geomorphology, 351 (2020) 106918, doi: 10.1016/j.geomorph.2019.106918.

[26] IAEA, Modelling of Marine Dispersion and Transfer of Radionuclides Accidentally Released from Land Based Facilities, International Atomic Energy Agency, Vienna, IAEA TECDOC Series, ISSN 1011–4289, no. 1876, 2019.

[27] C.O. Horita, P.C.C. Rosman, Lagrangian model for shallow water bodies contaminant transport, J. Coastal Res., 39 (2006) 1610–1613.

[28] J.T. Kirby, R.A. Dalrymple, F. Shi, Combined Refraction/Diffraction Model, 2002.

[29] S.P. Pereira, Modelagem da qualidade bacteriológica das águas costeiras de Fortaleza (Nordeste do Brasil), Tese (Doutorado), Departamento de Engenharia Hidráulica e Ambiental, Universidade Federal do Ceará, 2012.

[30] R.A.G. Silva, S.P. Pereira, P.C.C. Rosman, Numerical Modelling of the Coastal Circulation and Nearshore Currents on the Coast of Fortaleza – CE, XXII Simpósio Brasileiro de Recursos Hídricos, Florianópolis, Brazil, 2017.

[31] P. Palomar, J.L. Lara, I.J. Losada, Near field brine discharge modelling part 2: validation of commercial tools, Desalination, 290 (2012) 28–42.

[32] A. Purnama, H.H. Al-Barwani, T. Bleninger, R.L. Doneker, CORMIX simulations of brine discharges from Barka plants, Oman, Desal. Water Treat., 32 (2011) 329–338.

[33] A. Inan, Modeling of Hydrodynamics and Dilution in Coastal Waters, Water, 11 (2019) 83, doi: 10.3390/w11010083.